http://journal.uir.ac.id/index.php/JGEET

E-ISSN : 2541-5794
P-ISSN : 2503-216X

Journal of Geoscience,
Engineering, Environment, and Technology
Vol 9 No 1 2024

RESEARCH ARTICLE

The Investigation of the Dominant Direction of the Fault Structure Using the Radon Method at Mt. Pancar Geothermal Field

Faruk Afero [1], Varuliantor Dear [2], Asnawi Husin [3]

[1,2,3] *Space Research Center, National Research and Innovation Agency, Jakarta, Indonesia.*
[2] *School of Electrical Engineering and Informatics, Bandung Institute of Technology , Bandung, Indonesia*

Corresponding author : faru001@brin.go.id
Tel.:+62-813-1996-2849
Received: Oct 12, 2023; Accepted: Mar 7, 2024.
DOI: 10.25299/jgeet.2024.9.1.14556

Abstract

The Mt. Pancar geothermal field in Bogor, Indonesia, has been surveyed for radon in soil gas. There were 33 measurement points across the survey area that were separated by 100-200 meters. Through the radon method, this study aims to show the direction of the dominant fault structure based on the distribution of radon values in around observation area. The Radon concentration was measured by RAD 7 Electronic Radon Detector Durridge Company. The study showed the dominant structure was directed southwest-northeast, passing through the manifestation of the red crater. The result of radon soil gas survey performed highest radon concentration near the manifestations which was included survey area was about 10047 Bq/m^3. The manifestation was predicted to be controlled by the three faults in the Mt. Pancar geothermal field.

Keywords: Fault, Geothermal Exploration, Mt. Pancar, Radon Method.

1. Introduction

The Indonesian archipelago lies on the tectonic plate boundary between the Australian and Eurasian plates. Around the Indonesian archipelago, the heavier section of the Australian oceanic plate is subducting into the asthenosphere. The plate subduction process creates a partial melt of the plate material due to the numerous processes that occur in it. The partial melt process creates a magmatic chamber and a succession of volcanism above the subduction zone, resulting in a substantial geothermal potential for the Indonesian archipelago.

Mount Pancar is one of the Indonesian locations with significant geothermal potential. The presence of three crater-shaped surface manifestations (hot springs) demonstrates this possibility. Black crater, red crater, and white crater are the three surface expressions. The Mount Pancar area is highly important to investigate because the potential of the three craters is so great that it has not subsided for decades. The idea to map the Mount Pancar area and its environs (both locally and regionally) in order to confirm and define the direction of flow and the causes of present surface manifestations is an intriguing item to investigate. One of them is to identify fault lines that influence manifestations on Mount Pancar, as well as general indicators of places with larger concentrations that are suited for drilling geothermal steam using the radon method, because there is a considerable link between Radon and fault traces.

A fracture area is defined by features that cause geothermal manifestations, such as surface faults and subterranean faults. Meteoric water flowed into the ground through recharged areas, and when it came into contact with hot igneous rocks at depth, it heated up to produce a hot fluid. Convection would carry it to the surface due to its higher temperature and lighter mass. When fluid flows up and accumulates in high porosity places with impervious layers, geothermal reservoirs occur. Permeable zones in the reservoir, such as faults or cracks, could allow liquids to rise to the surface. Faults, which play a significant role in fluid transmission, transport geothermal fluid from reservoir to surface. Geothermal energy exploration is mostly concentrated on zones with high permeability, such as fault zones and reservoirs. To research geothermal fields, a permeable zone, such as a fault, must be characterized in detail and properly.

Geothermal field permeable zones can be detected using the Radon method, which is inexpensive, accurate, and easy to apply (Haerudin, 2020). As of 1984, it has become increasingly popular (Gingrich, 1984). A long-established method for detecting tectonic faults has been using radon (Rn) concentration in soil gas, especially for determining active faults and conducting earthquake studies (Inceöz et al., 2006), (Moussa and El Arabi, 2003) (Al-Hilal and Al-Ali, 2010), (Lombardi and Voltattorni, 2010), (Papastefanou, 2010), (Richon et al., 2010), and (Wang et al., 2013). Geothermal exploration has been aided by radioactivity measurements of Radon, commonly known as the Radon method, which is based on mineral exploration techniques, particularly Uranium exploration (238-U). It is the main source of radon (222-Rn). The number of studies has been conducted on the use of Radon gas in the exploration of geothermal fields, including (López et al., 1987) in Mexico to find the source of geothermal energy and (Chavarría et al., 2008) in the Las Pailas Costarika geothermal zone; and (Karingithi, 2010) conducted geochemical and Radon studies in Arus and Bogoria geothermal zones. As Radon enriches and migrates upward in fault zones, anomalous Radon concentrations can be observed above active fault zones (Ioannides et al., 2003) and (Swakoń et al., 2005). The use of radon measurement also has been proven successful

in determining active faults in numerous regions in Vietnam (Xuan et al., 2020).

Radioactivity is measured as a parameter to determine the study area's features. The use of radon as an indicator of concealed uranium reserves has been intensively investigated. This method, in conjunction with geoelectric methods, can be used to locate a fault or fracture zone. The radon method is commonly employed in geochemical methods. Radon method has been also successful as an effective way to detect hidden faults as in (Fu et al., 2005). Moreover, a qualitative analysis of radon counts in some geothermal prospects in Mexico was conducted as described in (Balcazar et al., 2010). In the meantime, in Indonesia, radon has been used as a geochemical tool in the Ungaran geothermal field for geothermal exploration (Nguyen et al., 2012) and (Haerudin, 2020) determined of fault that conect and control three manifestations in the southern part of the Rajabasa geothermal area by radon survey. Using a similar strategy but different instruments and sites, specifically the Mount Pancar geothermal area, based on the distribution of radon levels in the surrounding area, this study intends to show the direction of the major fault structure. Based on this, we expect that our research will help to enhance and supplement existing research on radon approaches used in geothermal field exploration.

2. Geological and Geochemical Setting

The Bogor area's geology was formed by the collision action of the Eurasian Continental Plate (northern, granitic) and the Indo-Australian Ocean Plate (southern, basaltic). The collision zone generates a trench-like shape in which various rocks accumulate, including deep sea sedimentary rocks (pelagic sediments), metamorphic rocks, and igneous rocks with alkaline to ultrabasic compositions (ophiolite).

The Bogor Zone is located south of the Jakarta Coastal Plain and runs approximately 40 kilometers from west to east, beginning in Rangkasbitung, Bogor, Subang, Sumedang, and terminating in Bumiayu. The Bogor Zone is a convex anticlinorium to the north in the direction of the west-east fold axis. The anticlinorium's core is made up of strata of Miocene rock, while the flanks are made up of Pliocene-Pleistocene rock. There are also various intrusive morphologies in the Bogor Zone, such as bosses. The rocks are turbidite layers of sandstone, clay, and breccia, with hypabyssal intrusions, conglomerates, and volcanic deposit material. Aside from that, limestone lenses with thick accumulations of Neogene deposits emerge.

The Bogor Sheet's geological structure consists of faults, folds, lineaments, and joints found in Tertiary (Oligocene, Miocene, and Pliocene) to Quaternary rocks. Tertiary volcanic formations on Mount Pancar and Quaternary volcanic formations on Mount Panisan serve as basements for Tertiary sedimentary formations in the Bogor Sheet Area (Fig. 1). Faults are divided into strike-slip and normal faults, and they commonly trend north-south, southwest-northeast, and northwest-southeast. Anticlines and synclines that trend southwest-northeast, west-east, and northwest-southeast were discovered. Joints typically form in Quaternary andesite rocks.

According to (van Bemmelen, 1970), the Bogor Zone was a deep sea basin at the beginning of the Oligocene marked by the occurrence of flysh deposits, which are marine deposits with volcanic rock inserts. Following this, volcanic activity was accompanied by subsidence, culminating in the creation of multiple underwater volcanoes around the beginning of the Miocene, which generated andesitic and basaltic deposits.

Mt. Pancar's geological structure was assumed to be dominated by the structure in the northwest-southeast direction. Hot springs, warm soil, and rock changes were surface manifestations in this geothermal area, which were controlled by the fault system beneath. Hot springs with a neutral pH were discovered in the red crater, as well as sintered silica. There were outcrops of light brown soil in the area around the base camp, and then silicified rocks deriving from igneous rocks altered by hydrothermal activity not far from the base camp. This change happened at temperatures ranging from 250°C to 350°C and was impacted by meteoric water and magma. Despite its dull white hue, this rock was compact, with no hollow voids and high-resistance silica. Carbonate sinter, which is dark brown in color, hollow and not hard, with a sharp surface structure that generates stratification or layers, can be found near the red crater hot spring. This bicarbonate sinter was formed from deposits from hot springs. Mount Pancar's geothermal potential area can be classified as having "low to moderate geothermal resources" based on this information.

The geochemical survey was conducted in two locations, the red and black craters, by monitoring the temperature of the two craters and observing the rock modification that happened surrounding the craters. There was a rock modification, specifically sintered silica, which is a chemical compound generated from the mineral silica (SiO_2). The recorded temperature in the red crater was 60°C, with the ambient temperature at the time being 29°C. Sintered silica is a silvery yellow silica precipitate on the surface. Typically found near hot springs and geyser openings spewing neutral water (chloride water). Silvery silica terraces (silica sinter terrace or sinter platform) formed around hot springs if the flow rate of hot water was not too high. The existence of sintered silica implies that the fluid surrounding it was taken from a reservoir fluid, specifically chloride water, as evidenced by the magnitude of the observed pH in the neutral red crater area (pH=6.8). The surface manifestation of water-dominated geothermal systems is sintered silica. There was also argillic alteration originating from basalt rocks around this crimson crater. In the dark crater area, the measured temperature was 48°C, the pH was 6.9, and the ambient temperature was 28°C. Not far away, there was an outcrop of scoria lava rock. Scoria is fantastic. Developed from pyroclastic lava rocks ejected by volcanoes. The presence of these rocks suggests the presence of hot lava flow from Mount Pancar. Mount Pancar is a water-dominated geothermal system with low to moderate geothermal potential, according to geochemical data.

3. Radon Migration Mechanisms

The two main modes of radon movement in the subsurface are diffusion and convection. Before radioactive decay, radon atoms migrated through these methods. Radon is released as it diffuses into a fluid in the rock. This is one of the primary processes for the release of radon from mineral grains. Radon gas was generated by the decay of radium and disseminated in the fissures of rocks and soil, eventually becoming part of the air near the earth's surface and tenuous near depth, where it originated.

Convection is a transport mecanism fluid (liquid or gas) to move and bring a radon, which can carry information about the geological environment. As stated in (Tanner, 1980), 222-Rn cannot be transported from the depth to the surface by diffusion alone, but also by convection. Convective transport mechanism can be used to explain

how radon can migrate at a significant distance. With a thermal gradient of 30°C/km, radon can be transported through soil or gas through convection (Fleischer et al., 1980) which results in vertical distances of 100 meters for air or water in sand with hydraulic conductivity ($K > 3.10^{-7}/cm^2$), and up to 300 meters for $K > 3.10^{-8}/cm^2$ for sand, soil, and high-permeability sandstone within the range of basal permeability ($10^{-5} - 10^{-9}/cm^2$). Fluid convection caused by thermal subterranean is a possible way for radon to be transported in areas with higher permeability than normal. When hot fluid from the geothermal area reacts with elements found in magmatic rocks, such as uranium, Radium, a daughter element, rises to the surface through cracks or faults.

Radon was chosen for exploration since it has a suitable half-life and is found in magmatic rocks derived from the decay of 238-U series, while thoron decay series is derived from thorium. Radon is a unique element in the chain of radioactive uranium decay, and can be detected in very low concentrations, making it a basis for highly sensitive geochemical methods. Radon is used as a tracer element because it can represent the thermodynamic activity, indicate active faults and fractures, and show recent geothermal activity (Al-Tamimi and Abumurad, 2001), (Moussa and El Arabi, 2003), (Xuan et al., 2020), and (Sato, 2003). Radon can be used to indicate fracture zones and high heat flow areas because it is soluble in water. 222-Rn is a natural tracer used in hydrothermal geothermal field. It is carried to the surface by convection.

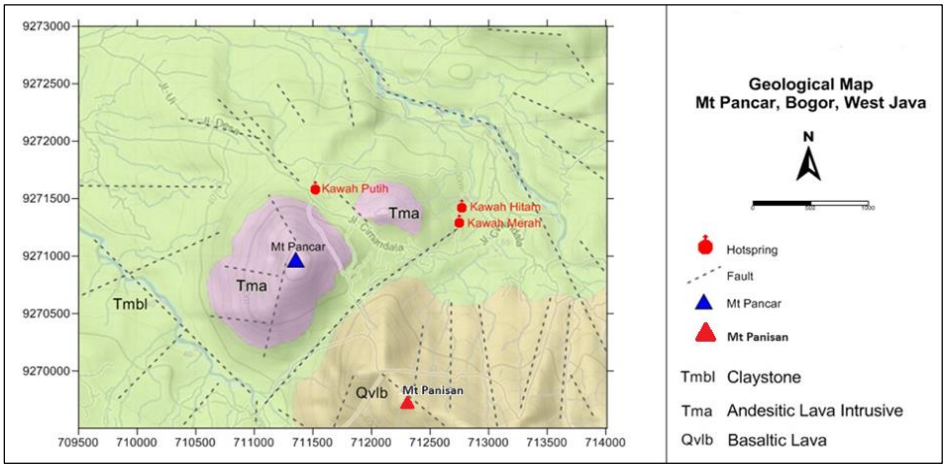

Fig. 1. Geological map of the Mt. Pancar geothermal prospect area. Mount Pancar's geological characteristics include Tertiary volcanic formations and Quaternary volcanic deposits on Mount Panisan, which underlie tertiary sedimentary strata as basement.

Table 1. Acquisition data of radon survey at Mt.Pancar Bogor, West Java.

Station	Coordinate			Radon (Bq/m^3)		Thoron (Bq/m^3)		Temp	Humidity
	X	Y	Z	Result	SD	Result	SD	(°C)	(%)
Pt 36	712748	9271297	405	10047	737	12400	1130	27,1	7
Pt 38	712923	9271419	361	459	187	2730	552	38,9	7
Pt 39	712997	9271484	376	1480	287	4100	658	39,9	7
Pt 37	712840	9271359	367	3050	400	1510	442	29,8	7
Pt 48	713152	9271469	429	542	194	1950	466	39,5	7
Pt 40	713081	9271538	414	875	237	3040	567	37,4	7
Pt 35	712666	9271241	502	164	134	1180	369	31,3	7
Pt 34	712597	9271185	499	109	127	1010	344	30,7	6
Pt 33	712524	9271125	491	2400	362	4940	711	28,6	6
Pt 04	712514	9271630	397	460	175	1380	395	26,8	8
Pt 12	712578	9271539	393	2460	358	3720	622	28,6	7
Pt 20	712649	9271445	387	2480	360	7040	845	31	7
Pt 28	712690	9271380	386	318	164	505	264	29,5	6
Pt 44	712859	9271252	388	497	183	2830	548	33,8	7
Pt 52	712882	9271138	401	1240	271	4200	698	36,5	7
Pt 60	712931	927153	414	329	166	855	325	31,6	7
Pt 61	713000	9271158	400	9640	698	7520	887	31,9	6
Pt 53	712928	9271206	453	3470	437	11k5	1080	33,8	7
Pt 45	712890	9271300	403	446	194	491	281	34,4	7
Pt 21	712711	9271525	399	4360	487	8670	942	28,3	7
Pt 29	712779	9271439	425	2330	371	7530	877	27,4	6
Pt 06	712714	9271758	352	2450	368	10k6	1030	29,5	7
Pt 15	712800	9271709	336	774	221	1970	469	30,4	7
Pt 23	712882	9271641	340	4580	489	5430	751	30,1	7
Pt 22	712778	9271564	349	2510	374	5780	773	30,1	6
Pt 46	712960	9271449	374	6870	604	15k2	1250	34,4	7
Pt 55	713121	9371317	401	4170	479	5390	757	31,6	6
Pt 54	713050	9274231	437	4800	513	13k6	1180	28,9	6
Pt 50	712731	9271042	432	8280	683	7280	928	26,4	6
Pt 43	712696	9271175	426	682	254	1440	465	26,4	6
Pt 26	712536	9271253	467	7590	646	12k5	1160	25,5	6
Pt 19	712547	9271398	431	4560	503	7590	901	25,2	6
Pt 27	712632	9271325	428	600	246	1360	409	24,6	6

4. Data and Methodology

Radon concentrations were tested using a DURRIDGE RAD7 Company radon detector, which was supported by

LEMIGAS, Indonesia. The alpha detector is used by the DURRIDGE RAD7. Using semiconductors, solid-state detectors convert alpha radiation directly into electrical impulses. Furthermore, the energy of each alpha particle may be electronically calculated. By knowing which isotope created the radiation, this approach may discriminate old radon from new radon, radon from thoron, and signal from noise. This technology, known as alpha spectrometry, enables sniffing or grab-sampling (Opondo and Sims, 2012). This test measures the amount of radon in the space for 15 minutes, produces the radon sample value, the thoron sample value, the humidity, and the environmental temperature. The data recorded was processed using Surfer Software 12 to show the contour map of radon counting and ratio of radon and thoron (Table 1).

5. Result and Discussion

The survey area was roughly 4.95 km^2, and 33 observation stations with 100-200m spacing were chosen. The measurement time for radon is 15 minutes, and the output includes radon value, thoron value, humidity, and environmental temperature. The manifestations covered in the data were red craters and black craters. The minimum radon concentration is 109 Bq/m^3, the maximum is 10047 Bq/m^3, with standard deviations of 127 Bq/m^3 and 737 Bq/m^3 correspondingly. The survey discovered a significant concentration in manifestation zones, with 2330 Bq/m3 in Black Crater and 10047 Bq/m^3 in Red Crater. The geometric mean value (average) plus the standard deviation is used to calculate the threshold value. Near the manifestation zones, the standard deviation values were 371 Bq/m^3 and 737 Bq/m^3, respectively. This approach detects a concentration anomaly in soil gas data. The value in Black Crater is lower than in Red Crater, but it is still greater than the standard deviation value. It could be caused by the clay overburden.

The data is displayed as a contour map in Fig. 2. A contour map is shown, with three dashed lines indicating high anomaly. Lines A, B, and C were characterized as faults that connected and governed geothermal manifestations. Regardless matter how deep the geothermal reservoir is, the faults allow fluid to move from there to the surface. High radon anomalies may suggest an increased permeability, indicating that radon is rapidly moving to the surface before decaying into daughter products.

Faults aid in gas transportation by increasing the permeability of the rock and assisting geothermal fluid flow up to the surface. The larger the value of the radon-to-thoron ratio on a fault, as shown in Fig.3, the deeper the fault is assumed to be. This is due to the fact that the deeper the fault, the more radon and thoron that can escape from the earth's bowels to the surface, yet thoron has a significantly shorter half-life than radon, which is just around 4 minutes. As a result, when it reaches the earth's surface, the amount of thoron remaining will be far lower than the amount of radon. As can be shown in Fig.3, the highest radon-to-thoron ratio was found around the manifestations.

Furthermore, the fluid migrating upward from deep sources is affected by other elements such as the level of cracking rock and the soil's ability to absorb water through the rocks. Figure 4 depicts the deepest structure controlling the manifestation and direction of radon structures for determining which one was the deepest structure controlling the manifestation and direction of radon structures.

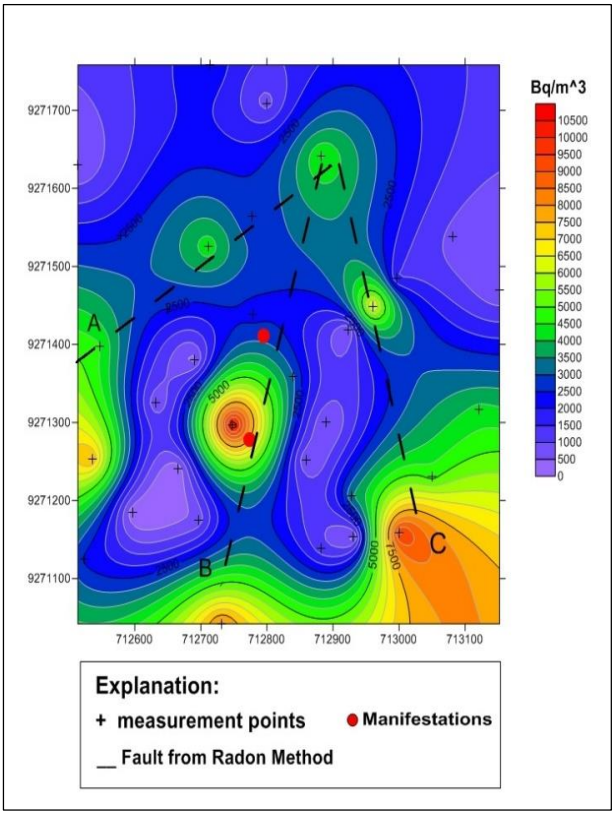

Fig.2. Contour map of radon counting. Three dashed lines indicate a high level of abnormality. Lines A, B, and C were designated as faults that linked and governed geothermal manifestations.

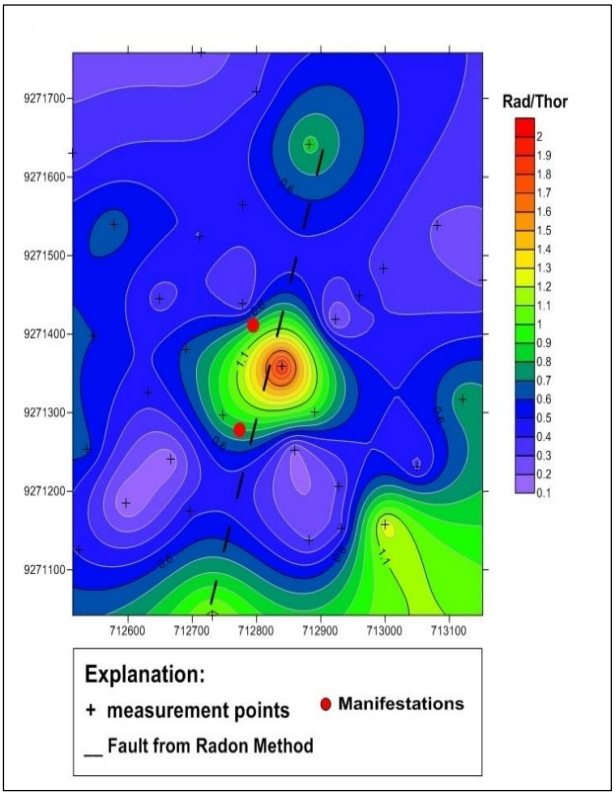

Fig 3. Contour map of ratio radon and thoron. The highest radon-to-thoron ratio was discovered near manifestations.

According to Fig.4, The orientation of the structure controlling these manifestations has been indicated by the findings of the radon survey. According to the survey data,

a powerful structure dominates the appearance of manifestations on Mt. Pancar, which is a southwest-northeast trending fault. This result is further supported by the overlay of Mt. Pancar's geological map, which indicates that the direction of the impending fault (white line) similarly points to the southwest-northeast.

Ground geological surveys are particularly difficult to use to locate faults in the geothermal field. Volcanoes are generated by complicated forces due to the complex factors influencing the structure of the area. The geological study predicted two manifestations connected by a straight line based on the assumption that the manifestations were governed by the presence of faults. Meanwhile, radon discharged from depth on the surface revealed that there is a fault in this area. The issue comes when there are a few sites with high radon concentrations that do not form a line. Other data or procedures should be provided to verify the existence and direction of the defect. Some methods that can be used are resistivity, SP (Self Potential), and remote sensing. The use of many methodologies will almost likely make the results of the observations more persuasive.

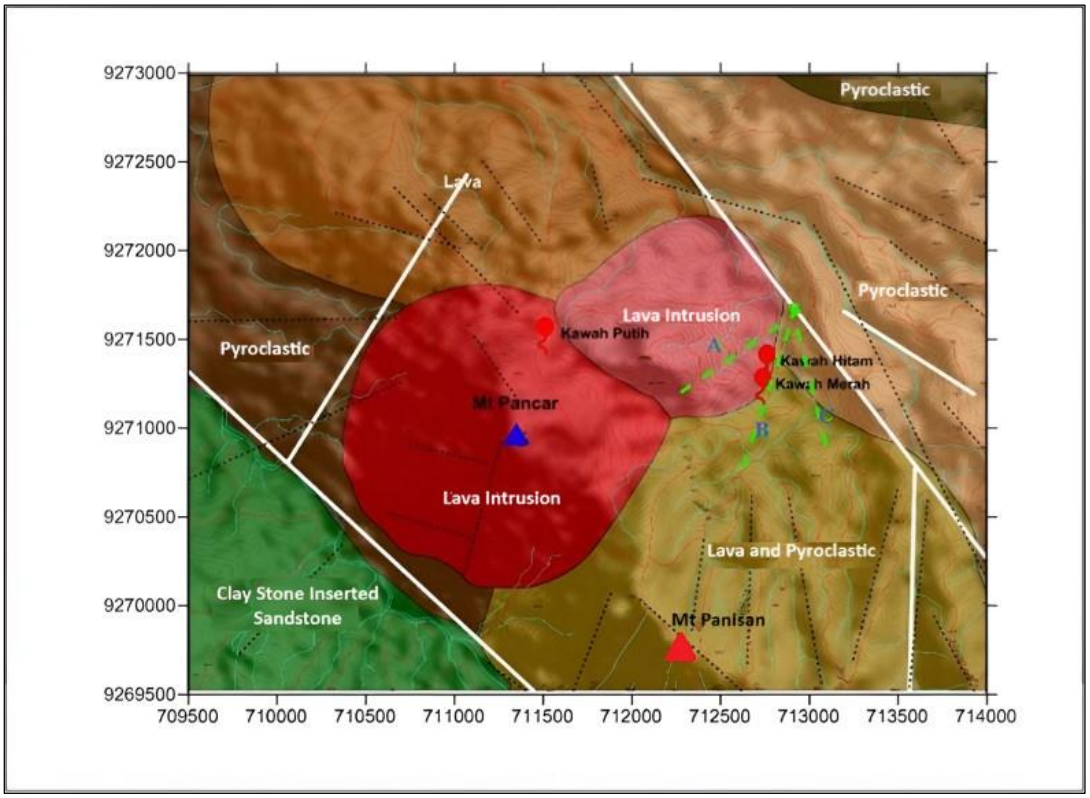

Fig 4. Radon survey overlaid with a geological map: determine the dominant structure controlling manifestation. The appearance of manifestations on Mt. Pancar, which is a southwest-northeast trending fault, is dominated by a tremendous structure.

6. Conclusion

A radon survey conducted in Mt. Pancar, Bogor, West Java, revealed that the greatest radon concentration of 10047 Bq/m^3 was found around the red crater manifestation, and the lowest radon concentration was found to be 109 Bq/m^3. High radon concentrations were discovered near the manifestation, including the survey area. The manifestations were controlled by three nearby faults, one of which was identified as the deepest structure via a contour map of the radon-to-thoron ratio. The radon survey demonstrates the fault structure's direction from southwest to northeast, with a radon distribution value greater than the surrounding observation region.

Acknowledgements

We would like to express our acknowledgements for the support of the DURRIDGE RAD7 equipment from LEMIGAS which was used during geothermal field observation survey activities on Mt. Pancar.

References

Al-Hilal, M., Al-Ali, A., 2010. The role of soil gas radon survey in exploring unknown subsurface faults at Afamia B dam, Syria. Radiat. Meas. 45, 219–224. https://doi.org/https://doi.org/10.1016/j.radmeas.2010.01.018

Al-Tamimi, M.H., Abumurad, K., 2001. Radon anomalies along faults in North of Jordan. Radiat. Meas. 34, 397–400. https://doi.org/10.1016/S1350-4487(01)00193-7

Balcazar, M., A, L., M, H., H, F., Pena, P., 2010. Use of Environmental Radioactive Isotopes in Geothermal Prospecting.

Chavarría, L., Torres, Y., Rodriguez, A.W., Molina, F., 2008. Soil Gas Radon Measurement as a Tool to Identify Permeable Zones at Las Pailas Geothermal Area, Costa Rica.

Fleischer, R.L., Hart, H.R., Mogro-Campero, A., 1980. Radon emanation over an ore body: Search for long-distance transport of radon. Nucl. Instruments Methods 173, 169–181. https://doi.org/https://doi.org/10.1016/0029-554X(80)90584-4

Fu, C.-C., Yang, T., Walia, V., 2005. Reconnaissance of soil gas composition over the buried fault and fracture zone

in southern Taiwan. Geochem. J. 39, 427–439. https://doi.org/10.2343/geochemj.39.427
Gingrich, J.E., 1984. Radon as a geochemical exploration tool. J. Geochemical Explor. 21, 19–39. https://doi.org/https://doi.org/10.1016/0375-6742(84)90032-3
Haerudin, N.H.N., 2020. A Soil Gas Radon Survey to Determine Fault at Southern Part of Rajabasa Geothermal Field, Lampung Indonesia. Int. J. Eng. Technol. IJET-IJENS 13.
Inceöz, M., Baykara, O., Aksoy, E., Doğru, M., 2006. Measurements of soil gas radon in active fault systems: A case study along the North and East anatolian fault systems in Turkey. Radiat. Meas. 41, 349–353. https://doi.org/10.1016/j.radmeas.2005.07.024
Ioannides, K., Papachristodoulou, C., Stamoulis, K., Karamanis, D., Pavlides, S., Chatzipetros, A., Karakala, E., 2003. Soil gas radon: a tool for exploring active fault zones. Appl. Radiat. Isot. 59, 205–213. https://doi.org/https://doi.org/10.1016/S0969-8043(03)00164-7
Karingithi, C., 2010. The geochemistry of Arus & Bogoria geothermal prospects, in: ARGEO-C1 Conference. pp. 1–20.
Lombardi, S., Voltattorni, N., 2010. Rn, He and CO2 soil gas geochemistry for the study of active and inactive faults. Appl. Geochemistry 25, 1206–1220. https://doi.org/10.1016/j.apgeochem.2010.05.006
López, A., Gutiérrez, L., Razo, A., Balcázar, M., 1987. Radon mapping for locating geothermal energy sources. Nucl. Instruments Methods Phys. Res. Sect. A Accel. Spectrometers, Detect. Assoc. Equip. 255, 426–429. https://doi.org/https://doi.org/10.1016/0168-9002(87)91142-9
Moussa, M.M., El Arabi, A.G.M., 2003. Soil radon survey for tracing active fault: A case study along Qena-Safaga road, Eastern Desert, Egypt. Radiat. Meas. 37, 211–216. https://doi.org/10.1016/S1350-4487(03)00039-8
Nguyen, P., Harijoko, A., Itoi, R., Unoki, Y., 2012. Water geochemistry and soil gas survey at Ungaran geothermal field, central Java, Indonesia. J. Volcanol. Geotherm. Res. s 229–230, 23–33. https://doi.org/10.1016/j.jvolgeores.2012.04.004
Opondo, K.M., Sims, K., 2012. Electronic Radon Detector User Manual.
Papastefanou, C., 2010. Variation of radon flux along active fault zones in association with earthquake occurrence. Radiat. Meas. 45, 943–951. https://doi.org/https://doi.org/10.1016/j.radmeas.2010.04.015
Richon, P., Klinger, Y., Tapponnier, P., Li, C.-X., Woerd, J., Perrier, F., 2010. Measuring radon flux across active faults: Relevance of excavating and possibility of satellite discharges. Radiat. Meas. 45, 211–218. https://doi.org/10.1016/j.radmeas.2010.01.019
Sato, J., 2003. Natural radionuclides in volcanic activity. Appl. Radiat. Isot. 58, 393–399. https://doi.org/10.1016/S0969-8043(02)00317-2
Swakoń, J., Kozak, K., Paszkowski, M., Gradziński, R., Łoskiewicz, J., Mazur, J., Janik, M., Bogacz, J., Horwacik, T., Olko, P., 2005. Radon concentration in soil gas around local disjunctive tectonic zones in the Krakow area. J. Environ. Radioact. 78, 137–149. https://doi.org/10.1016/j.jenvrad.2004.04.004
Tanner, A.B., 1980. Radon migration in the ground: a supplementary review. United States.
van Bemmelen, R.W., 1970. The Geology of Indonesia. U.S. Government Printing Office.
Wang, X., Li, Y., Du, J., Zhou, X., 2013. Correlations between radon in soil gas and the activity of seismogenic faults in the Tangshan area, North China. Radiat. Meas. 60. https://doi.org/10.1016/j.radmeas.2013.11.001
Xuan, P.T., Duong, N.A., Chinh, V. Van, Dang, P.T., Qua, N.X., Pho, N. Van, 2020. Soil Gas Radon Measurement for Identifying Active Faults in Thua Thien Hue (Vietnam). J. Geosci. Environ. Prot. 08, 44–64. https://doi.org/10.4236/gep.2020.87003

© 2024 Journal of Geoscience, Engineering, Environment and Technology. All rights reserved. This is an open access article distributed under the terms of the CC BY-SA License (http://creativecommons.org/licenses/by-sa/4.0/).